Regulation of phosphatidylinositol 3–kinase by polyisoprenyl phosphates in neutrophil-mediated tissue injury

Caroline Bonnans,[1] Koichi Fukunaga,[1] Raquel Keledjian,[3] Nicos A. Petasis,[3] and Bruce D. Levy[1,2]

[1]Department of Medicine and [2]Center of Experimental Therapeutics and Reperfusion Injury, Brigham and Women's Hospital and Harvard Medical School, Boston, MA 02115
[3]Department of Chemistry, University of Southern California, CA 90089

Neutrophils play a central role in host defense, inflammation, and tissue injury. Recent findings indicate a novel role for polyisoprenyl phosphates (PIPPs) as natural down-regulatory signals in neutrophils. The relationship between PIPPs and neutrophil early activating signals, such as phosphoinositides, has not been previously determined. Here, we establish presqualene diphosphate (PSDP) as an endogenous PIPP regulator of phosphatidylinositol 3–kinase (PI3K). In human neutrophils, leukotriene B_4 (LTB_4) triggered rapid decreases in PSDP and reciprocal increases in PI3K activity. In addition, PSDP was identified by gas chromatography/mass spectrometry in p110γ–PI3K immunoprecipitates obtained 30 s after LTB_4, indicating a physical interaction between PSDP and PI3K in activated neutrophils. Moreover, PSDP (0.4–800 pmol) directly inhibited recombinant human p110γ-PI3K activity. During an experimental model of lung injury and inflammation, a reciprocal relationship was also present in vivo for lung PSDP and PI3K activity. To investigate its therapeutic potential, we developed a new PSDP structural mimetic that blocked human neutrophil activation and mouse lung PI3K activity and inflammation. Together, our findings indicate that PSDP is an endogenous PI3K inhibitor, and suggest that in inflammatory diseases characterized by excessive neutrophil activation, PIPPs can serve as structural templates in a novel antineutrophil therapeutic strategy to limit tissue injury.

CORRESPONDENCE
Bruce D. Levy:
blevy@partners.org

Innate immune responses are essential to host defense, yet if unchecked can lead to tissue injury and illness (1). PMN are the primary initial immune effectors of acute inflammation, and these cells use as many as fifty toxins for microbial killing in phagocytic vacuoles (2). Incomplete closure of phagolysosomes or aberrant extracellular release of reactive oxygen species (ROS), granule components, lipid mediators, hypochlorous acid, and other potentially toxic PMN products to surrounding tissues contribute to injury in several human diseases, including the devastating clinical entities of acute lung injury (ALI) and acute respiratory distress syndrome (ARDS) for which no disease-remitting therapy is currently available (3).

To prevent an overexuberant inflammatory response and limit damage to the host, PMN activation programs need to be tightly controlled (1). Select membrane-derived lipid mediators have recently been described as autacoid regulators of PMN functional responses in acute inflammation (4). One of these classes of antiinflammatory membrane lipids involves isoprenoid metabolism. Immune regulatory roles for isoprenoids are emphasized by the hyper-IgD and periodic fever syndrome that results from low polyisoprenyl phosphate (PIPP) levels secondary to defective mevalonate kinase activity (5). Recently, we identified a novel PIPP signaling pathway in PMN (6). One of its components is presqualene diphosphate (PSDP), present in freshly isolated human PMN in nanomolar quantities at baseline (i.e., 1.7 nmol/10^7 cells) (6). PMN exposure to the chemoattractant and secretagogue leukotriene B_4 (LTB_4) initiates transient activation of this PIPP signaling pathway with conversion of PSDP to its monophosphate form, presqualene monophosphate (PSMP). PSDP carries biological

The online version of this article contains supplemental material. Supplemental material can be found at: http://doi.org/10.1084/jem.20052143

activity as a potent counterregulatory mediator that prevents ROS generation (6, 7). In sharp contrast, PSMP is >100-fold less active than PSDP for inhibition (6, 7). Thus, incoming positive signals for PMN (e.g., LTB_4) initiate rapid degradation and inactivation of an inhibitory lipid signal (i.e., PSDP) coincident with cell responses (e.g., ROS generation). PSDP levels quickly return to baseline in a time frame that parallels cellular deactivation. Intracellular targets for PSDP to control PMN activity remain to be elucidated. Select PSDP structural mimetics are also active in vivo, dampening mouse responses to zymosan A–induced peritonitis (8).

In addition to PSDP remodeling, LTB_4 also initiates phosphatidylinositol 3–kinase (PI3K) activation in PMN to promote NADPH oxidase assembly and ROS production (9, 10). Phosphoinositide signaling initiated by PI3Ks is a critical early event in PMN responses, such as phagocytosis (11) and chemotaxis (12), and contributes to ALI pathogenesis (13). Because LTB_4 initiates PMN PI3K activation and PIPP remodeling, we hypothesized that these signaling events were related in the regulation of PMN responses. Here, we report that PI3K activity and PSDP remodeling are linked during PMN activation and deactivation with direct inhibition of PI3K by PSDP to limit PMN responses and lessen the severity of experimental lung inflammation.

RESULTS AND DISCUSSION

PSDP and PI3K regulate LTB_4-triggered O_2^- release by human PMN

To determine if PSDP and PI3K regulate LTB_4-stimulated responses, we exposed freshly isolated human PMN to a new structural PSDP mimetic (Fig. 1 A) or a potent and specific inhibitor of PI3K activity (LY294002) before LTB_4. A marked increase in the rate of O_2^- generation was observed within seconds after LTB_4 addition that was transient, slowing considerably by 60 s (Fig. 1 B). The presence of either PSDP mimetic (100 nM) or PI3K inhibitor (3 μM) markedly blocked O_2^- generation. Exposure to LTB_4 (10 min) induced 1.6 ± 0.3 nmol $O_2^-/10^6$ PMN (as compared with vehicle 0.5 ± 0.1 nmol $O_2^-/10^6$ PMN; $P < 0.01$). Both the PSDP mimetic and PI3K inhibitor led to >50% inhibition of LTB_4-triggered O_2^- generation (0.8 ± 0.3 nmol/10^6 PMN and 0.7 ± 0.2 nmol/10^6 PMN, respectively; $P < 0.05$) (Fig. 1 C). The PSDP mimetic concentration in these experiments (i.e., 100 nM) was 1,000-fold lower than its critical micellar concentration (CMC) (~100 μM; Fig. S1, at http://www.jem.org/cgi/content/full/jem.20052143/DC1). To verify that the observed inhibition was not secondary to micelle formation and sequestration of the lipid agonist LTB_4, in the next experiments, there was pretreatment with the mimetic, a wash, and stimulation with LTB_4. Although this extra step reduced total ROS generation in response to LTB_4, the PSDP mimetic still led to a >50% decrease (71.2 ± 27.7% inhibition, $n = 4$). Together, these results indicate that human PMN activation by LTB_4 is highly dependent on PI3K activity and can be inhibited by a new PSDP structural mimetic.

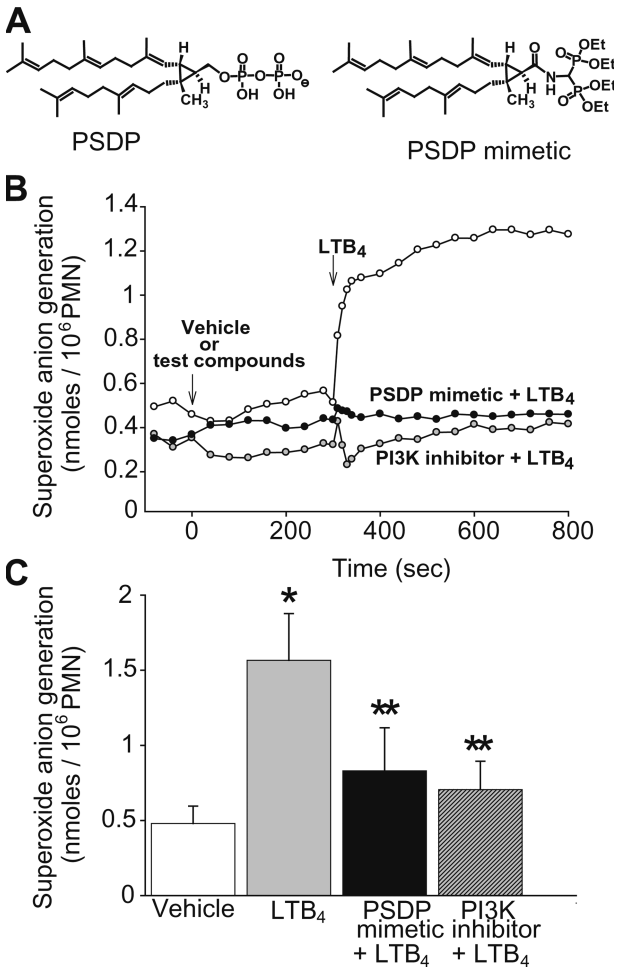

Figure 1. Superoxide anion generation by human PMN is regulated by PI3K and PSDP. (A) Structure of PSDP and a new amido PSDP structural mimetic (CS ChemDraw software). (B) Freshly isolated human PMN were exposed to the PSDP mimetic (100 nM) (●), a PI3K inhibitor (3 μM) (◎), or vehicle (○) before LTB_4 (100 nM) and O_2^- generation was determined. Results are representative for $n = 3$. (C) Total O_2^- generation was also determined for LTB_4-activated PMN (10 min) in the presence or absence of the test compounds (mean ± SEM; $n = 4$ from separate PMN donors; *, $P < 0.01$ as compared with vehicle; **, $P < 0.05$ as compared with LTB_4).

Relationship between PI3K activity and PSDP during PMN activation

To determine if PSDP remodeling and PI3K activation were related, we first examined their kinetics in human PMN after exposure to LTB_4. Because G protein–coupled receptors can activate class IA and IB PI3Ks (10), we measured PIP_3 formation in vitro by members of these PI3K classes. After LTB_4, p110γ–PI3K activity in PMN rapidly increased (within 5 s), reached a maximum rate of activity by 20 s, and then declined to basal levels within 30 s (Fig. 2 A, representative for $n = 3$). LTB_4 also rapidly stimulated p85-based PI3K activity in PMN, but at lower levels than p110γ–PI3K. By 5 s, significant decrements were also evident in total PSDP levels (7.9 ± 1.2%; $P < 0.01$) (see supplemental

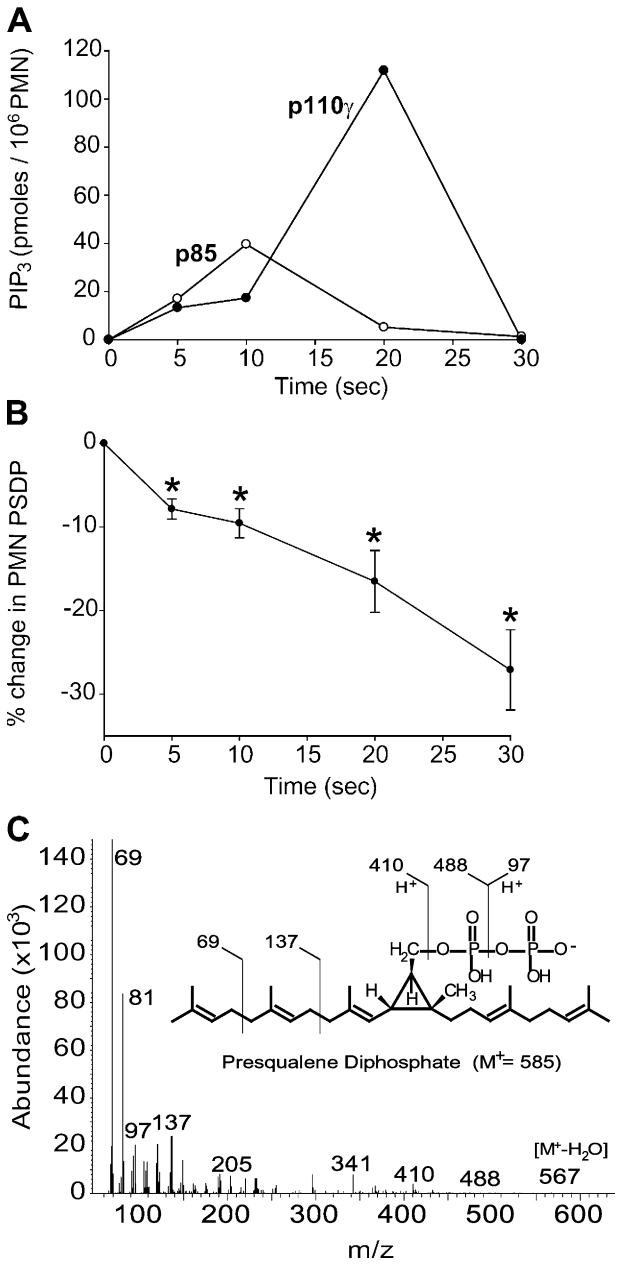

Figure 2. Relationship between PI3K activity and PSDP in activated human PMN. 5×10^6 PMN were exposed to 100 nM LTB_4 and both PI3K activity and PSDP levels were measured at timed intervals. (A) Representative time course ($n = 3$) in PMN lysates for p110γ- (●) and p85-based (○) PI3K activity. (B) PSDP levels in activated PMN were measured in parallel with PI3K. Values reported are the percentage of change in PSDP (mean ± SEM; $n = 4$, *, $P < 0.001$). (C) PMN were exposed to LTB_4 (100 nM, 37°C) for 30 s and p110γ–PI3K was isolated by immunoprecipitation with a specific antibody. Lipids were extracted from the immunoprecipitates and taken to GC/MS. Ions (m/z) present in materials bound to p110γ–PI3K were diagnostic for PSDP as noted in the inset.

Materials and methods, available at http://www.jem.org/cgi/content/full/jem.20052143/DC1) that progressed to 27.1 ± 4.8% reductions ($P = 0.001$) within 30 s (Fig. 2 B). These results indicate that LTB_4-triggered activation of PMN PI3K and PSDP remodeling was concurrent and temporally overlapped with initiation of ROS generation. Although both of these signaling events were rapid in onset, the kinetics for PI3K activation and deactivation differed from the time course for total PSDP remodeling during the initial 30-s interval. To determine if PSDP directly interacted with PI3K as its activity decreased, PMN were exposed to LTB_4 for 30 s and p110γ–PI3K was immunoprecipitated from cellular materials. Lipid extracts were performed and analyzed by gas chromatography/mass spectrometry (GC/MS) (6). Selective ion monitoring at m/z 137 (2 isoprenoid units) revealed a unique peak at 18.1 min in LTB_4-exposed PMN extracts. MS spectral diagnostic ions (Fig. 2 C), namely m/z 567 [$M^+ - (H_2O)$], 488 [$M^+ - (H_2PO_4)$], 410 [$M^+ - (HP_2O_7)$], 341 [$M^+ - (HP_2O_7) - 69$], 205 {$M^+ - [HP_2O_7] - 69 - [CH_2C(CH_3)CHCH_2 \times 2]$}, 137 [$C_{10}H_{17}$], 97 [$H_2P_2O_7$], 81 [$CH_2C(CH_3)CH(CH_2)_2 - H^+$] and 69 [base peak; $(CH_3)_2CCHCH_2$], were consistent with authentic PSDP in the PI3K immunoprecipitated material.

Direct inhibition of p110γ–PI3K by PSDP

Because PI3K activity and PSDP remodeling were both early signaling events in PMN with interaction between PSDP and p110γ–PI3K, next we questioned if PSDP could directly regulate PI3K activity. Recombinant human (rh) p110γ–PI3K activity was determined by PIP_3 formation in vitro in the presence of PSDP, PSMP, or the PI3K inhibitor LY294002. PIP_3 formation was significantly decreased by PSDP (800 pmol) with 94.7 ± 5.3% inhibition ($P < 0.001$) and a PI3K inhibitor (500 pmol) with 46.7 ± 6.7% inhibition ($P = 0.01$) (Fig. 3 A). PSDP inhibited p110γ–PI3K in a concentration-dependent fashion (Fig. 3 B). In sharp contrast, PSMP (8–800 pmol) did not significantly impact p110γ–PI3K activity. The IC_{50} for PSDP (38 pmol) had a stoichiometry with PI3K of ~9:1. These results indicate that PSDP is a potent direct inhibitor of p110γ–PI3K with a structure–activity relationship that suggests an important role for the diphosphate structure in PSDP's action on p110γ–PI3K activity. The LTB_4-mediated PMN remodeling of PSDP corresponds to an ~50 pmol change in PSDP/10^6 PMN, a decrease that is within the concentration range for regulation of p110γ–PI3K activity (Fig. 3 B). After cell activation, the percent change in total PSDP (i.e., 28%) is similar to the change in phosphatidylinositol (17%) that occurs in activated PMN membranes (14). Collectively, our new findings indicate that receptor-mediated agonists for PMN remodel PSDP in time-frames and amounts consistent with functional impact on PI3K activity and cellular responses.

PSDP remodeling in vivo during tissue injury and inflammation

Because PI3K activity occupies a central role in regulating PMN activation during lung injury and inflammation (13), next we determined PSDP remodeling in vivo in mouse lungs during an experimental model of mild ALI secondary

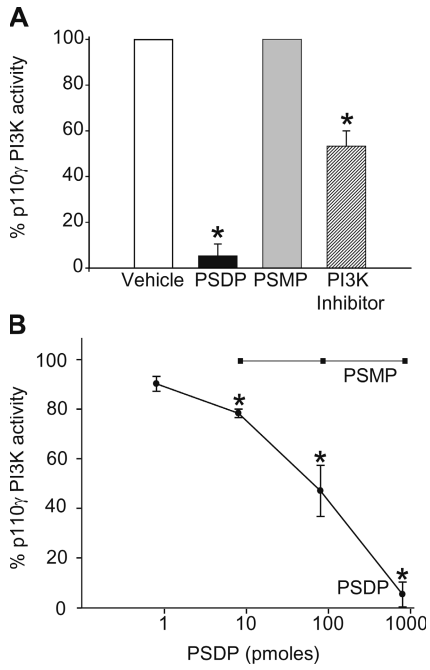

Figure 3. PSDP directly blocked PI3K activity. (A) rhp110γ–PI3K activity was determined in the presence or absence of PSDP (800 pmol), PSMP (800 pmol), or a PI3K inhibitor (500 pmol). (B) Concentration response for the impact of PSDP (●) or PSMP (■) on rhp110γ–PI3K activity (mean ± SEM; $n = 3$; *, $P < 0.05$ as compared with vehicle).

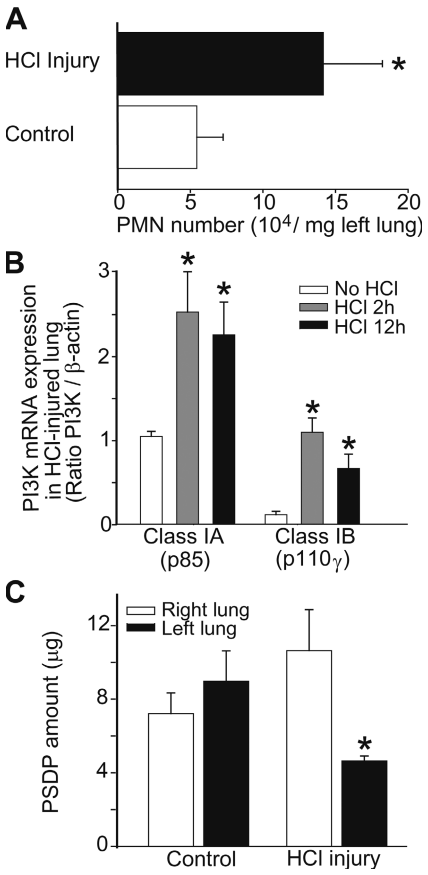

Figure 4. ALI induced PMN infiltration, PI3K, and PSDP remodeling. (A) 12 h after HCl-initiated ALI, PMN accumulation was determined by MPO activity in lung homogenates ($n = 5$; *, $P = 0.002$). (B) Semi-quantitative RT-PCR for p85 and p110γ–PI3K mRNA expression in the injured lungs 2 and 12 h after HCl instillation ($n = 3$; *, $P < 0.05$). (C) PSDP levels were measured in lung lipid extracts with or without HCl-initiated injury (12 h; mean ± SEM; $n = 3$–4; *, $P < 0.05$).

to aspiration of gastric acid (15), which is a common clinical event (3). To simulate acid aspiration, hydrochloric acid (HCl) (0.1 N, pH = 1.5) was selectively instilled into the animals' left lungs (15). Lung PMN infiltration was maximal 12 h after HCl injury (14.2 ± 1.8 vs. 5.5 ± 0.8 × 10^4 PMN/mg lung; $P < 0.01$) (Fig. 4 A). Expression of class IA and IB PI3Ks in mouse lungs were both increased at 2 and 12 h after HCl (Fig. 4 B). Lungs were removed and lipid extracts were prepared for PSDP determination. Of interest, despite increased PMN numbers, PSDP levels were significantly lower in the left lungs of HCl-injured mice (4.6 ± 0.3 μg PSDP vs. 9.0 ± 1.6 μg PSDP in control lungs; $P < 0.02$). These results indicate that experimental lung injury led to decrements in PSDP concomitant with increased PMN, suggesting an inverse relationship in vivo between lung PSDP and inflammation.

PSDP mimetic blocks PMN infiltration and PI3K activity

To determine if PSDP can block pulmonary inflammation and PI3K in vivo, we administered a PSDP structural mimetic (0.8 μg/mouse, i.v.) or vehicle 15 min before HCl instillation into the left main-stem bronchus. PSDP markedly reduced lung PMN 12 h after injury (Fig. 5 A). Tissue morphometry on LY-6G–stained histological sections (for identification of mouse PMN) revealed significant inhibition with the PSDP mimetic (46.8 ± 7.1% LY-6G staining [HCl] vs. 18.8 ± 5.8% LY-6G staining [HCl plus PSDP mimetic]; $P < 0.05$) (Fig. 5 B). In view of the prominent class IA PI3K lung expression that increased markedly after ALI (Fig. 4 B), we next determined class IA PI3K activity after acid injury in the presence or absence of the PSDP mimetic. HCl injury induced significant increases in lung PI3K activity in p85 immunoprecipitates (0.59 ± 0.17 PIP_3/mg lung with HCl vs. 0.05 ± 0.02 pmol PIP_3/mg lung with PBS; $P < 0.05$). Administration of the PSDP mimetic blocked the HCl-induced increase in class IA PI3K activity to near basal levels (0.05 ± 0.01 pmol PIP_3/mg lung; $P < 0.05$) (Fig. 5 C). Thus, PSDP can regulate PMN activation, tissue accumulation, and total PI3K activity in vivo during experimental acid-initiated ALI.

During acute inflammation, PI3Ks orchestrate several cellular responses for host defense, including PMN ROS generation (12). Befitting its central role in cell activation, several mechanisms are in place to restrain PI3K activity (16–18). Previous reports have suggested a link between decreased PIPP formation and increased PI3K (19, 20). Results presented here are the first to demonstrate direct inhibition of PI3K by a PIPP and inverse relationships between PI3K

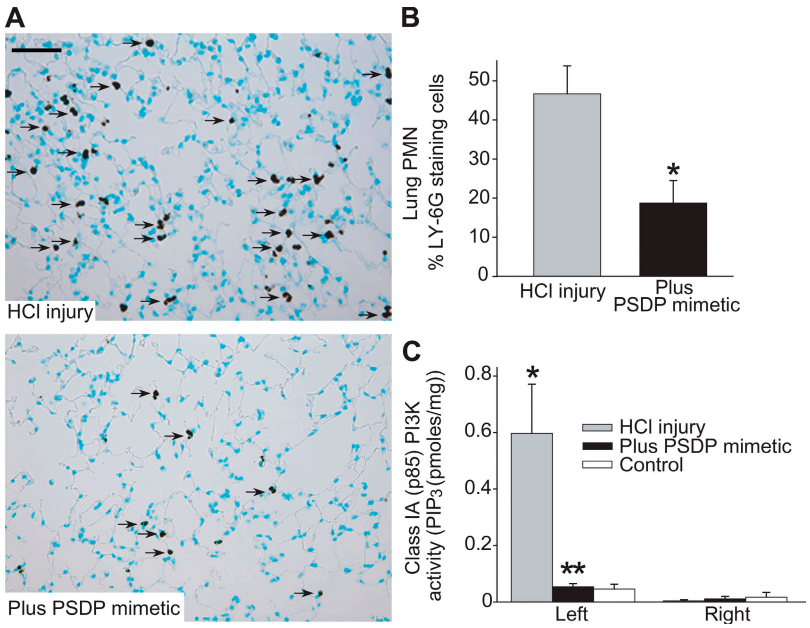

Figure 5. PSDP reduced acid-initiated ALI. (A) PSDP structural mimetic (0.8 μg/mouse) or vehicle was administered (i.v.) 15 min before HCl injury. 12 h after HCl instillation, histological specimens were prepared and mouse PMN were identified by LY-6G immunostaining (arrows). Bar, 100 μm. (B) Tissue morphometry was performed to determine the percentage of LY-6G staining cells in mouse lungs ($n = 4$ measurements in each group; *, $P < 0.05$ as compared with HCl-injured left lung). (C) Class IA (p85-based) PI3K activity was determined in lung lysates after ALI. Data are mean ± SEM. $n = 3$; *, $P < 0.05$ as compared with control; **, $P < 0.05$ as compared with HCl-injured lung.

activity and PSDP levels both in vitro and in vivo. In addition, PSDP bound to p110γ–PI3K in activated PMN and potently inhibited rhp110γ-PI3K in vitro and a PSDP structural mimetic blocked PI3K activity in vivo. Together, these new findings support a signaling relationship between PI3K and PIPPs in the regulation of leukocyte functions during inflammation.

Pivotal regulatory properties have been ascribed to isoprenoids. For example, polyisoprenyl glycolipids form antigen complexes with CD1 to activate T cells (21), and cholesterol is critical to PMN cell membrane organization and polarization in response to chemotactic stimuli (22). Although PIPPs are appreciated as cholesterol biosynthetic intermediates, PSDP is also present in cells, such as human PMN, that cannot use it for cholesterol biosynthesis because they lack squalene cyclase and other mixed function oxidase activities (23). There are now several lines of evidence to support a role for PSDP as a counterregulatory signal in PMN functional responses. PSDP is a constituent of PMN cell membranes (20), and receptor activation leads to rapid and transient PIPP remodeling. PSDP is a potent and direct inhibitor of phospholipase D (PLD) with at least two interaction domains on human PLD1b for PSDP (8). PSDP also interacts with Src-homology 2 (SH2) domains on the adaptor protein Grb2 (24) and blocks NADPH oxidase assembly in a cell-free assay (6). PSDP displays anti-PMN properties in vitro and in vivo, and PSDP structural mimetics are able to dampen leukocyte-driven inflammation (8). Here, we have identified PI3K as a new target for regulation by PSDP. The physical interaction between PI3K and PSDP and absence of regulatory proteins in our in vitro system indicate that PSDP can directly inhibit p110γ–PI3K. Similar to PLD (8), the diphosphate moiety of PSDP was also important for PI3K inhibition, and the stoichiometry suggests multiple potential sites for PSDP and PI3K interaction. Both class IA and IB PI3Ks translocate to membranes via interactions with Ras that is activated, in part, via isoprenylation (25). These shared isoprenoid moieties with PSDP may provide additional sites of interaction outside the PI3K catalytic center. Of interest, PSDP and PI3K are present in resting PMN in complementary intracellular locations (cell membranes and cytosol, respectively), and both translocate to intracellular organelles upon cell activation (20, 26).

Activated PMN contribute to the development and severity of tissue injury during inflammatory illnesses such as ALI. No specific therapy is currently available to modulate the inflammatory response to airway injury from acid and protect the lung in ALI. PI3K is an important enzyme in the proinflammatory PMN signaling program of ALI, as p110γ–PI3K deficiency dampens the severity of endotoxin-induced ALI (13). In addition to PMN, PI3Ks are also activated during ALI in lung-resident cells (27) and both endothelial cell and PMN PI3Ks contribute to PMN accumulation in the lung (28). Select lipid mediators, namely lipoxin A_4 (LXA_4), inhibit PI3K in structural cells (29). LXA_4 signaling also promotes resolution of experimental ALI (15) and inhibits PMN activation by LTB_4 in a postreceptor manner, in part by blocking PSDP remodeling (7). Here, PSDP levels were

decreased in acid-injured lungs and a novel PSDP mimetic blocked PI3K, PMN ROS generation, and PMN accumulation in the lung. Because the PSDP mimetic was administered intravenously, regulation of cells other than PMN may have also contributed to the marked inhibition of leukocyte trafficking after acid injury.

In conclusion, the ability of PSDP and a new PSDP mimetic to directly inhibit PMN early intracellular activating signals, such as PI3K, and to lessen the inflammation associated with experimental ALI provides insight into new mechanisms for in vivo protection from excess PMN-driven inflammation and tissue injury. Together, our findings suggest that PIPP signaling pathways, and specifically PSDP, can serve as natural templates for the design of new therapeutic strategies in inflammatory diseases.

MATERIALS AND METHODS

Materials. PSDP and PSMP were isolated from human PMN or prepared by total organic synthesis (8). The bisphosphonate PSDP structural mimetic, tetraethyl presqualene carboxamido-methylene-diphosphonate was prepared from presqualene carboxylic acid. All synthetic compounds were characterized by NMR spectroscopy.

Human PMN incubations. Peripheral blood was obtained by venipuncture from healthy volunteers who denied taking any medications for at least 2 wk and had given written informed consent to a protocol approved by Brigham and Women's Hospital's Human Research Committee. PMN were isolated from whole blood as described previously (6). Freshly isolated PMN ($1–5 \times 10^6$ PMN/ml HBSS plus 1.6 mM $CaCl_2$) were incubated (5 min, 37°C) in the presence of 3 μM LY294002, 100 nM PSDP mimetic, or vehicle (0.1% ethanol), then exposed to LTB_4 (100 nM) in the presence of 7 mg/ml cytochrome c. This concentration of LTB_4 was chosen because it initiates PMN NADPH oxidase assembly (7) and is similar to amounts measured in vivo at sites of acute inflammation (30). In some incubations, PMN in HBSS without calcium were exposed to PSDP mimetic or vehicle, pelleted by centrifugation (700 *g*, 3 min), and resuspended in HBSS plus 1.6 mM $CaCl_2$ without PSDP before the addition of agonist. Superoxide anion generation was determined (37°C) as superoxide dismutase-inhibitable cytochrome c reduction by monitoring (550 nm) at 5-s intervals in a continuously flowing water-bath–jacketed cassette or after timed incubations. For PSDP identification, PMN ($50–100 \times 10^6$ cells/ml) were activated (LTB_4 100 nM, 30 s) before disruption by N_2 cavitation (350 psi, 20 min, 4°C). Remaining intact cells and nuclei were pelleted (500 *g*, 10 min, 4°C) and supernatants were used for immunoprecipitation with anti-p110γ−PI3K (4°C). After overnight incubation, washed protein A agarose (60 μl) was added and incubated for 2 h at 4°C. After several washes, the immunoprecipitates were saponified, lipids were extracted, and materials were analyzed by GC/MS (Hewlett-Packard) (6). Injections in 2–5 μl $CHCl_3$ were made onto a fused-silica capillary DB-17 column (30 mm, 0.25 mm i.d.) obtained from J&W. Scientific with helium as carrier gas and a column temperature program (150–260°C at 15°C per min^{-1}).

Measurement of class IA and IB PI3K activity. After immunoprecipitation with either an anti-p85 or anti-p110γ–PI3K selective antibody, PI3K activity from PMN and lung homogenates was determined by PIP_3 formation in vitro using a competitive ELISA (Echelon Biosciences Inc.). For recombinant purified PI3K enzyme, activity was determined by a luminescent kinase assay (Kinase-Glo; Promega) that quantitated decrements in ATP by kinase utilization. rh p110γ–PI3K (4 pmol/reaction) was exposed (15 min, 37°C) to PSDP or PSMP (0.4–800 pmol) followed by 25 μg L-α-phosphatidylinositol and 1 μM ATP and allowed to react for 90 min at room temperature. Incubations were stopped with 50 μl of Kinase-Glo reagent and incubated an additional 10 min at room temperature. Luminescence was measured with a FLx800 microplate luminometer (Bio-Tek Instruments, Inc.).

Experimental model of ALI. All animal protocols were approved by the Harvard Medical Area Animal Institutional Review Board. Acid (0.1 N HCl, pH = 1.5, 50 μl) was instilled intratracheally into the left lung of anesthetized mice (FVB, male, 10–12 wk; Charles River Laboratories) (15). A PSDP mimetic (0.8 μg in 100 μl 0.9% saline) or vehicle (1% ethanol) was administered by tail vein 15 min before HCl instillation. After 12 h, lungs were removed, prepared for MPO (15) or PI3K assay, or were fixed in IHC zinc buffer and paraffin embedded for immunostaining with LY-6G (1:50 dilution). Area and number of positively staining cells was measured with National Institutes of Health Image software and percentage of positive cells/area calculated.

Statistical analysis. Results are expressed as the mean ± SEM. Statistical significance of differences was assessed by Student's *t* test and one-way analysis of variance. $P < 0.05$ was set as the level of significance.

Online supplemental material. Fig. S1 shows the CMC determination for the PSDP mimetic and related compounds. Further information on materials and experimental protocols are supplied as the supplemental Materials and methods. Online supplemental material is available at http://www.jem.org/cgi/content/full/jem.20052143/DC1.

The authors would like to acknowledge the contributions of Dr. C.N. Serhan to the development of the PSDP mimetic and for his critical review of the manuscript. We also thank Dr. M.A. Perrella and members of the Brigham and Women's Hospital Lung Biology Center and Histopathology Core Laboratory for their assistance with the experimental models of ALI.

This work was supported in part by the NIH (HL68669 and NIDCR Specialized Research Center grant no. DE016191), and fellowships from La Fondation de la Recherche Médicale, Pfizer, and Uehara Memorial Research Foundation.

The authors have no conflicting financial interests.

Submitted: 24 October 2005
Accepted: 27 February 2006

REFERENCES

1. Nathan, C. 2002. Points of control in inflammation. *Nature*. 420: 846–852.
2. Weiss, S.J. 1989. Tissue destruction by neutrophils. *N. Engl. J. Med*. 320: 365–376.
3. Ware, L.B., and M.A. Matthay. 2000. The acute respiratory distress syndrome. *N. Engl. J. Med*. 342:1334–1349.
4. Gilroy, D.W., T. Lawrence, M. Perretti, and A.G. Rossi. 2004. Inflammatory resolution: new opportunities for drug discovery. *Nat. Rev. Drug Discov*. 3:401–416.
5. Drenth, J.P.H., and J.W.M. van der Meer. 2001. Hereditary periodic fever. *N. Engl. J. Med*. 345:1748–1757.
6. Levy, B.D., N.A. Petasis, and C.N. Serhan. 1997. Polyisoprenyl phosphates in intracellular signalling. *Nature*. 389:985–990.
7. Levy, B.D., V.V. Fokin, J.M. Clark, M.J. Wakelam, N.A. Petasis, and C.N. Serhan. 1999. Polyisoprenyl phosphate (PIPP) signaling regulates phospholipase D activity: a 'stop' signaling switch for aspirin-triggered lipoxin A 4. *FASEB J*. 13:903–911.
8. Levy, B.D., L. Hickey, A.J. Morris, M. Larvie, R. Keledjian, N.A. Petasis, G. Bannenberg, and C.N. Serhan. 2005. Novel polyisoprenyl phosphates block phospholipase D and human neutrophil activation in vitro and murine peritoneal inflammation in vivo. *Br. J. Pharmacol*. 146:344–351.
9. Karlsson, A., J.B. Nixon, and L.C. McPhail. 2000. Phorbol myristate acetate induces neutrophil NADPH-oxidase activity by two separate signal transduction pathways: dependent or independent of phosphatidylinositol 3-kinase. *J. Leukoc. Biol*. 67:396–404.
10. Ito, N., T. Yokomizo, T. Sasaki, H. Kurosu, J. Penninger, Y. Kanaho, T. Katada, K. Hanaoka, and T. Shimizu. 2002. Requirement of phosphatidylinositol 3-kinase activation and calcium influx for leukotriene B4-induced enzyme release. *J. Biol. Chem*. 277:44898–44904.

11. Scott, C.C., W. Dobson, R.J. Botelho, N. Coady-Osberg, P. Chavrier, D.A. Knecht, C. Heath, P. Stahl, and S. Grinstein. 2005. Phosphatidylinositol-4,5-bisphosphate hydrolysis directs actin remodeling during phagocytosis. *J. Cell Biol.* 169:139–149.
12. Hirsch, E., V.L. Katanaev, C. Garlanda, O. Azzolino, L. Pirola, L. Silengo, S. Sozzani, A. Mantovani, F. Altruda, and M.P. Wymann. 2000. Central role for G protein-coupled phosphoinositide 3-kinase gamma in inflammation. *Science.* 287:1049–1053.
13. Yum, H.K., J. Arcaroli, J. Kupfner, R. Shenkar, J.M. Penninger, T. Sasaki, K.Y. Yang, J.S. Park, and E. Abraham. 2001. Involvement of phosphoinositide 3-kinases in neutrophil activation and the development of acute lung injury. *J. Immunol.* 167:6601–6608.
14. Serhan, C.N., M.J. Broekman, H.M. Korchak, A.J. Marcus, and G. Weissmann. 1982. Endogenous phospholipid metabolism in stimulated neutrophils differential activation by FMLP and PMA. *Biochem. Biophys. Res. Commun.* 107:951–958.
15. Fukunaga, K., P. Kohli, C. Bonnans, L.E. Fredenburgh, and B.D. Levy. 2005. Cyclooxygenase 2 plays a pivotal role in the resolution of acute lung injury. *J. Immunol.* 174:5033–5039.
16. Gout, I., G. Middleton, J. Adu, N.N. Ninkina, L.B. Drobot, V. Filonenko, G. Matsuka, A.M. Davies, M. Waterfield, and V.L. Buchman. 2000. Negative regulation of PI 3-kinase by Ruk, a novel adaptor protein. *EMBO J.* 19:4015–4025.
17. Harrington, L.S., G.M. Findlay, and R.F. Lamb. 2005. Restraining PI3K: mTOR signalling goes back to the membrane. *Trends Biochem. Sci.* 30:35–42.
18. Kwak, Y.G., C.H. Song, H.K. Yi, P.H. Hwang, J.S. Kim, K.S. Lee, and Y.C. Lee. 2003. Involvement of PTEN in airway hyperresponsiveness and inflammation in bronchial asthma. *J. Clin. Invest.* 111:1083–1092.
19. Dimmeler, S., A. Aicher, M. Vasa, C. Mildner-Rihm, K. Adler, M. Tiemann, H. Rutten, S. Fichtlscherer, H. Martin, and A.M. Zeiher. 2001. HMG-CoA reductase inhibitors (statins) increase endothelial progenitor cells via the PI 3-kinase/Akt pathway. *J. Clin. Invest.* 108: 391–397.
20. Levy, B.D., and C.N. Serhan. 2000. Polyisoprenyl phosphate signaling: topography in human neutrophils. *Biochem. Biophys. Res. Commun.* 275: 739–745.
21. Moody, D.B., M.R. Guy, E. Grant, T.Y. Cheng, M.B. Brenner, G.S. Besra, and S.A. Porcelli. 2000. CD1b-mediated T cell recognition of a glycolipid antigen generated from mycobacterial lipid and host carbohydrate during infection. *J. Exp. Med.* 192:965–976.
22. Pierini, L.M., R.J. Eddy, M. Fuortes, S. Seveau, C. Casulo, and F.R. Maxfield. 2003. Membrane lipid organization is critical for human neutrophil polarization. *J. Biol. Chem.* 278:10831–10841.
23. Shechter, I., A.M. Fogelman, and G. Popjak. 1980. A deficiency of mixed function oxidase activities in the cholesterol biosynthetic pathway of human granulocytes. *J. Lipid Res.* 21:277–283.
24. Levy, B.D., and C.N. Serhan. 2003. Polyisoprenyl phosphates: natural antiinflammatory lipid signals. *Cell. Mol. Life Sci.* 59:1–13.
25. Philips, M.R., M.H. Pillinger, R. Staud, C. Volker, M.G. Rosenfeld, G. Weissmann, and J.B. Stock. 1993. Carboxyl methylation of Ras-related proteins during signal transduction in neutrophils. *Science.* 259: 977–980.
26. Yu, W., J. Cassara, and P.F. Weller. 2000. Phosphatidylinositide 3-kinase localizes to cytoplasmic lipid bodies in human polymorphonuclear leukocytes and other myeloid-derived cells. *Blood.* 95:1078–1085.
27. Uhlig, U., H. Fehrenbach, R.A. Lachmann, T. Goldmann, B. Lachmann, E. Vollmer, and S. Uhlig. 2004. Phosphoinositide 3-OH kinase inhibition prevents ventilation-induced lung cell activation. *Am. J. Respir. Crit. Care Med.* 169:201–208.
28. Puri, K.D., T.A. Doggett, J. Douangpanya, Y. Hou, W.T. Tino, T. Wilson, T. Graf, E. Clayton, M. Turner, J.S. Hayflick, and T.G. Diacovo. 2004. Mechanisms and implications of phosphoinositide 3-kinase δ in promoting neutrophil trafficking into inflamed tissue. *Blood.* 103:3448–3456.
29. McMahon, B., C. Stenson, F. McPhillips, A. Fanning, H.R. Brady, and C. Godson. 2000. Lipoxin A4 antagonizes the mitogenic effects of leukotriene D4 in human renal mesangial cells. Differential activation of MAP kinases through distinct receptors. *J. Biol. Chem.* 275: 27566–27575.
30. Klein, A., A. Talvani, D.C. Cara, K.L. Gomes, N.W. Lukacs, and M.M. Teixeira. 2000. Stem cell factor plays a major role in the recruitment of eosinophils in allergic pleurisy in mice via the production of leukotriene B4. *J. Immunol.* 164:4271–4276.

Bonnans et al. http://www.jem.org/cgi/content/full/jem.20052143/DC1

SUPPLEMENTAL MATERIALS AND METHODS

LTB_4 was otained from Cayman Chemical; LY294002 was obtained from Cell Signaling Technology; dolichol monophosphate was obtained from American Radiolabeled Chemical, Inc.; o-dianisidine dihydrochloride, cytochrome *c*, and ATP were obtained from Sigma Chemical Co.; human p110γ PI3K was obtained from Alexis Biochemicals; L-α-phosphatidylinositol was obtained from Avanti Polar Lipids, Inc.; and anti-p110γ and anti-p85–PI3K antibodies were obtained from Upstate Biotechnology. IHC zinc buffer and mouse anti–LY-6G antibody were obtained from BD Biosciences.

PSDP determination.
The amount of PSDP was determined by densitometry (Scion Image software) after materials were saponified (10% KOH in methanol, 30 min, 37°C), extracted, and separated by TLC. Dolichol monophosphate (2 μg) was used as an internal control to correct for extraction losses.

P85 and p110γ-PI3K gene expression.
Total RNA was extracted from snap-frozen lungs and semi-quantitative gene expression was determined using specific primers for murine p85 (sense primer 5′-ACCCCAGTTTTTGTTGCTTG-3′, antisense primer 5′-CCTGCCCAACATTTAGTCCA-3′), p110γ PI3K (sense primer 5′-TTCTCGTGTGTCCACCATGT-3′, antisense primer 5′-CCTGGGCATCTCAGTGGTAT-3′), and β-actin (internal control). After electrophoresis, densitometry was performed using Scion Image software.

CMC measurement.
CMC was determined by light scattering (Levy, B.D., N.A. Petasis, and C.N. Serhan. 1997. *Nature*. 389:985–990). In brief, PSDP mimetic, the related PIPPs PSMP and farnesyl diphosphate (FDP), or L-α-phosphatidylinositol (PI) (10^{-9}–10^{-3} M) were added to HBSS containing 1.6 mM $CaCl_2$. After vortexing (30 s, room temperature) and sonication (30 s × 3, full power), materials were kept at room temperature for 30 min. For each compound, the relationship between absorbance at 762 nm (Abs 762 nm) and concentration was determined and the breakpoint in Abs 762 nm was taken as an estimate of the CMC (see Fig. S1).

www.jem.org/cgi/doi/10.1084/jem.20052143